LM-04K046
June 9, 2004

System Performance Projections for TPV Energy Conversion

P.F. Baldasaro, M.W. Dashiell, J.E. Oppenlander, J.L. Vell, P. Fourspring, K. Rahner, L.R. Danielson, S. Burger and E. Brown

System Performance Projections for TPV Energy Conversion

P. F. Baldasaro, M.W.Dashiell, J.E. Oppenlander, J.L. Vell, P. Fourspring, K. Rahner, L.R. Danielson, S. Burger, E. Brown

Lockheed Martin Corporation
Schenectady, NY 12301-1072

Abstract TPV technology has advanced rapidly in the last five years, with diode conversion efficiency approaching >30%, and filter efficiency of ~80%. These achievements have enabled repeatable testing of 20% efficient small systems, demonstrating the potential of TPV energy conversion. Near term technology gains support a 25% efficient technology demonstration in the two year timeframe. However, testing of full size systems, which includes efficiency degradation mechanisms, such as: non-uniform diode illumination, diode and filter variability, temperature non-uniformities, conduction/convection losses, and lifetime reliability processes needs to be performed. A preliminary analysis of these differential effects has been completed, and indicates a near term integrated system efficiency of ~15% is possible using current technology, with long term growth to 18-20%. This report addresses the system performance issues.

INTRODUCTION

The purpose of this report is to begin quantification of TPV system features that determine overall system conversion efficiency. Although significant progress has been made on filter and diode component technology, as demonstrated by small scale unit efficiency tests documented in References [1-3], these results do not include many of the loss factors associated with large scale generators. The results presented below represent an initial assessment of the loss factors to direct future analysis and testing, but do not reflect an optimized design at this point in time.

SIMULATION ASSUMPTIONS

While simple network case studies can be performed using basic circuit analysis and hardware experiments, computer-aided simulation of the TPV system and operating conditions is an invaluable tool for evaluating the many complex factors that influence larger scale TPV networks. In this work, a custom built simulation system that includes the electrical circuit analysis tool, Saber® (Synopsis, Inc.) is used to perform DC analysis of electrical networks having 480 series/parallel connected diodes. Individual diode electrical parameters were obtained from a database of five hundred ~0.5cm^2 InGaAsSb/GaSb (~0.52eV) single junction TPV diodes. Diode electrical parameters, measured under appropriate screening conditions are fit to equation-5 of [ref 4], where the definitions, as well as the statistical distributions, can be found in Table 1.

Simulated arrays of 8 parallel strings of 60 series-connected diodes (8×60) are populated with diodes described by the distributions given in Table I. Diode temperatures are assumed to be constant at 27°C. The nominal network output voltage is 12 volts at V_{max} and 8 amps at I_{max} (approximating a 950°C radiator).

Table I. Parameters of 0.52eV InGaAsSb Diodes used in the Studies

Diode Parameter	Units	Distribution Normal: (mean ± stand. dev) Triangular (min, mode, max)	Lower Bound	Upper Bound
Saturation Current Density (I_o/A)	A/cm^2	Triangular($2x10^{-5}$, $1.3x10^{-4}$, $6x10^{-4}$)	-	-
Series Resistance (R_s)	mΩ	Normal: 3 ±1	0.5	6.0
Ideality Factor (n)	-	Triangular (0.96,1.12,1.41)	-	-
Shunt Resistance (R_{sh})	Ω	Normal 35.0 ± 10.0	5.0	65.0
Light Generated Current Density (I_{light}/A)	A/cm^2	Normal 2.3 ± 0.1	2.0	2.6
Breakdown Voltage (V_b)	V	Normal: 0.20 ± 0.39	-1.5	2.0
Breakdown Parameter (b)	-	Normal: 6.0 ± 2.0	1.0	15.0

COMPONENT VARIABILITY AND SELECTION CRITERIA

It is convenient to define an overall diode figure of merit parameter (FOM) equal to the maximum output power from an individual diode: FOM = $I_{SC} \times V_{oc} \times FF$, which include the intrinsic diode variability from Table I. The FOM can be used to characterize the diode population as shown in the normalized distribution in Figure 1.

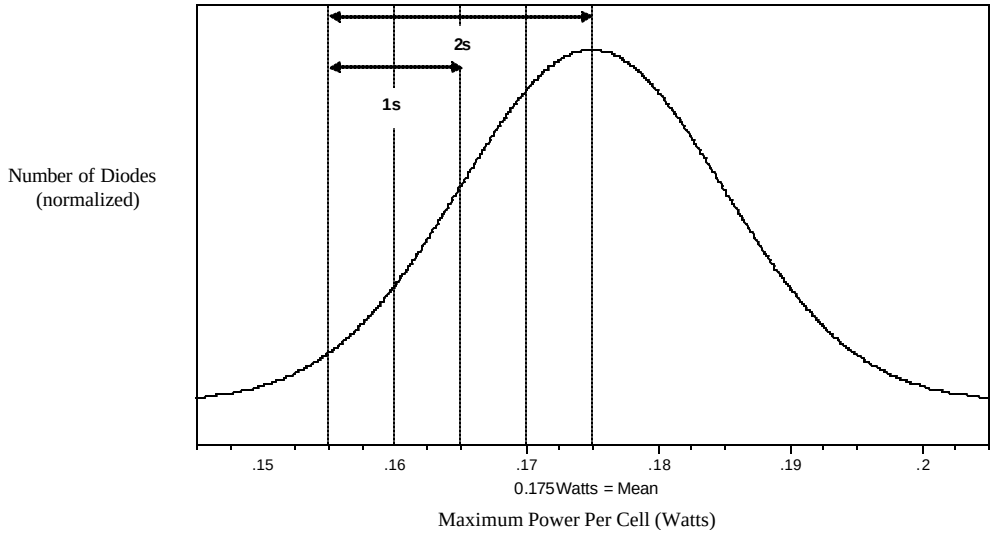

FIGURE 1. Normalized distribution and standard deviations (σ) of the FOM (maximum power) of the diodes used in the network analysis study. Measured power is taken from an illuminated electrical screening test of the individual diodes.

Small scale efficiency testing will typically reflect diodes having the highest FOM (~2σ above the mean) of the population. Cost, however, will dictate that a much larger fraction of the distribution be used in large scale generators. This study employs a commonly used selection practice that sets a minimum FOM cutoff for populating the TPV array. Figure 2 shows the simulated network output power as a function of the FOM cutoff criteria under uniform illumination. A diode cutoff of FOM=0.14W corresponds to the 8×60 array being randomly populated by nearly 100% of the distribution shown in Figure 1. The cutoff of FOM=0.175W corresponds to populating the 8×60 array only with the best performing half of the population. The decrease in power using the full population includes both the influence of (i) decrease in average FOM and (ii) the networking losses associated with interconnecting mismatched diodes. Assuming a cutoff of one standard deviation below the mean, this study estimates a ~10% relative loss in power/efficiency due to manufacturing/component

variability in large scale TPV generators compared to higher efficiencies quoted for small scale systems.

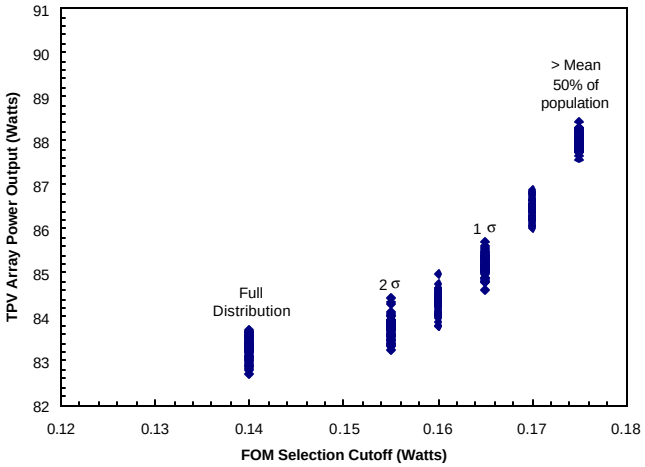

FIGURE 2. Simulated output power from a 8×60 array of 0.52eV InGaAsSb TPV diodes as a function of the FOM cutoff criteria. FOM cutoffs are also labeled in terms of standard deviation corresponding to the distribution of Figure 1.

NON-UNIFORM ILLUMINATION

For a TPV array operating in the presence of non-uniform illumination due, for example, to shadowing or a temperature gradient, the following losses will occur (i) reduced energy transfer to the diode from the hot side and (ii) increasing internal energy losses in the weakly-illuminated diode(s). A diode with low current output in a string results in a reverse voltage on the weak diode in order to match the current to the string value. To compensate for this loss in solar photovoltaics, often the connection of a bypass Zener diode in parallel with a shaded diode or substring artificially produces a very low breakdown voltage. This mitigates the network loss associated with substantial and diverse shading patterns encountered in space satellites [5]. TPV generators likewise are expected to experience some degree of non-uniform illumination due to temperature gradients, deposition, etc. Rather than incorporating additional bypass diodes, the diode architecture could be designed for low breakdown voltages in order to mitigate the network losses associated with non-uniform illumination.

ABRUPT ILLUMINATION GRADIENT

A diode's breakdown voltage determines the network voltage output that must be consumed to drive the string current through a weakly illuminated diode(s). Consequently, system losses from strong illumination non-uniformities will be sensitive to the breakdown voltage. A simplified current-voltage relation of the $\mathbf{j^{th}}$ diode in a series network can be described by equation (1).

$$i_j(v_j) = i_o\left\{\left(e^{v_j/nkT} - 1 - e^{-(v_j+V_b)/bkT}\right\} - i_{Light_j}\right. \qquad (1)$$

where each diode has the equivalent saturation current $\mathbf{i_o}$, ideality $\mathbf{n}$, and reverse breakdown parameters $\mathbf{V_b}$ and $\mathbf{b}$, ($kT=0.026eV$). Considering a series string of these N identical diodes, the string's output network electrical characteristics $\mathbf{I_{string}}$ and $\mathbf{V_{string}}$ can be determined by solution of equation (2):

$$V_{string}(I_{string}) = \sum_{i}^{N} \left[v_j(i_j = I_{string}) \right] \quad (2)$$

In a uniform illuminated string each diode will operate at the same voltage, thus the string's $(IV)_{string}$ curve is identical to the single cell characteristics, save for the series-scaling of voltage. If, however, the string is non-uniformly illuminated then $v_j \neq v_{j+1}$. The worst case scenario is one where a very weakly illuminated diode is driven to a large reverse voltage ($v_j << 0$) in order to maintain string current.

Figure 3a shows the calculated electrical output from a series string of 20 identical $1cm^2$ diodes when (i) all cells are uniformly illuminated ($i_{Light} \sim 3Amps$) and (ii) case of a single diode experiencing an abrupt reductions in i_{Light}. Because of the lower photocurrent generated in the shaded/obscured diode, a step appears in the string's IV characteristics when the network attempts to drive the string current beyond the i_{Light} of the shaded diode. The string current remains limited by the lowest value of i_{Light} (shaded) until that diode breaks down. The width (on the voltage scale) of the step corresponds to the network voltage that must be dropped across the single shaded diode in order to reach the breakdown voltage. If the shaded diode's breakdown voltage is larger than the string's available photovoltage then the network itself cannot drive the fully illuminated i_{Light} value under the string's short circuit conditions. Figure 3b shows experimental shading (approximately 50%) of a single diode within a 24 cell string of $0.5cm^2$ 0.52eV InGaAsSb TPV diodes under flash illumination. Experimentally, P_{max} decreased by 34% due primarily to this networking loss (i.e. the decrease of input optical power due to shading is only approximately 5%). The simple model used above and shown in Figure 3a fits well to the experiment (Figure 3b).

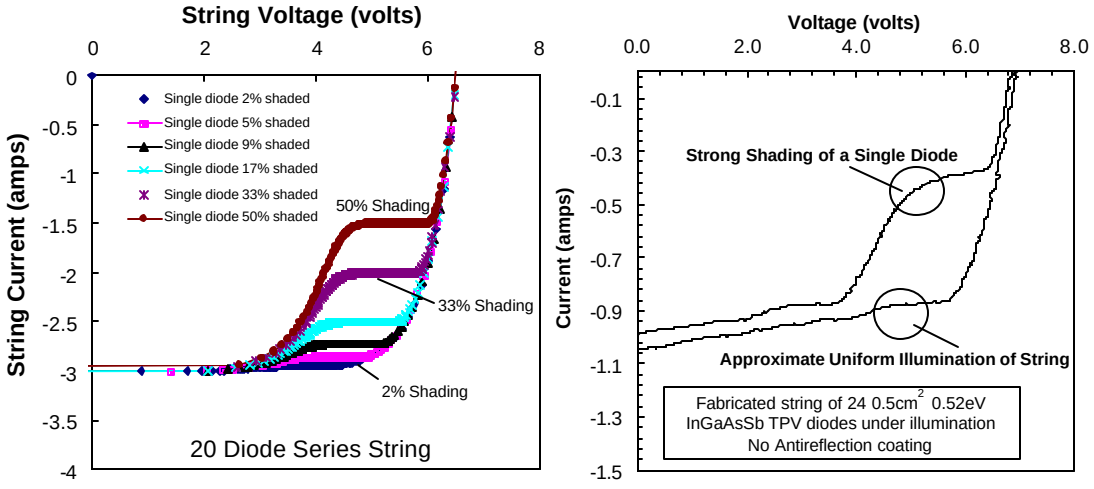

FIGURE 3. a) IV curves of a series string of 20 $1cm^2$ ideal diodes for various shading conditions of a single diode. b) Measured current voltage characteristics under (i) approximately-uniform and (ii) Approximately 50% shading of one diode in a series string of 24 $0.5cm^2$ InGaAsSb TPV diodes.

By adjusting the doping in the active regions of 0.52eV InGaAsSb TPV diodes, various reverse breakdown characteristics have been observed, without any degradation of the forward bias (power generating) electrical characteristics. Figure 4a shows a typical forward bias IV characteristic under uniform illumination for a $0.5cm^2$ 0.52eV InGaAsSb diode. Figure 4b shows measured reverse bias characteristics having a high breakdown voltage ($N_{emitter}=10^{17}cm^{-3}$, $N_{base}=10^{18}cm^{-3}$ labeled as A-High) and a low breakdown voltage ($N_{emitter}=2\times10^{18}cm^{-3}$,

$N_{base}=10^{18}cm^{-3}$ labeled C-Low). An intermediate case (close to our experimental mean) is modeled (labeled B-Medium).

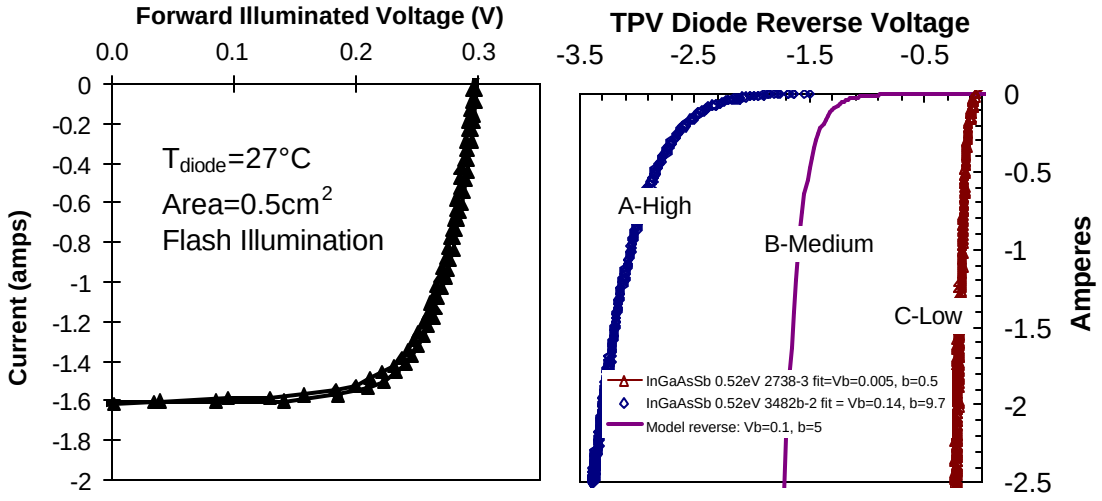

FIGURE 4 (a) Current-voltage curve for a 0.52eV InGaAsSb TPV diode under illumination. (b) Fig 4b shows simulated and experimental reverse breakdown data for 0.52eV InGaAsSb TPV diodes.

Figure 5 shows the influence of the different diode diode breakdown characteristics shown in figure 4b for the case of 50% shading across one diode within the series string. Uniform illumination is shown for reference.

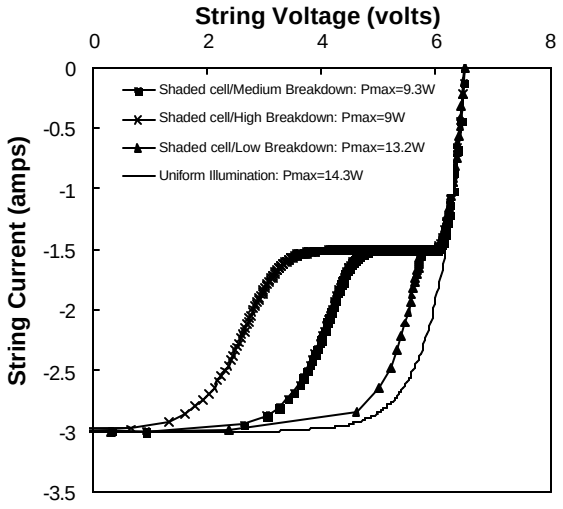

FIGURE 5. Calculated influence of breakdown characteristics on a 20-cell string (one diode in the string is 50% illuminated) for the three reverse characteristics shown in Figure 4b (high, medium, low). Also shown is the fully illuminated array (P_{max}=14.3Watts). Because of the power drop across the reverse-biased shaded cell the string P_{max} is reduced to 9, 9.3, and 13.2 Watts for the high, medium, low breakdown characteristics respectively.

Figure 5 shows a ~3V reverse voltage drops across the **High**-breakdown shaded diode corresponding to 37% network power decrease compared to the uniformly illuminated string. Under equivalent conditions, series strings having **Medium**-breakdown and **Low**-breakdown diodes indicate reverse voltage drops of ~1.5V and ~0.3V across the shaded diode respectively and network power losses of 35% and 8% respectively. Note that the majority of the power losses are due to network losses, not due to the decrease in available input power to the shaded cell (which corresponds only to a 2.5% decrease of radiant power).

WEAKLY VARYING TEMPERATURE GRADIENTS IN A 8´60 ARRAY

Based upon the discussion in Section IVa, a concern in TPV systems is the radiator temperature gradient, which will degrade the network performance because of the strong temperature dependence of emission power and limiting behavior of weakly illuminated diodes. This section presents a simulation of a continuous linear temperature gradient (parallel to the series strings) across the 8×60 TPV network using the distribution of diodes shown in Figure 1. The linear illumination gradient was varied from $\Delta T=0$ to $\Delta T\sim100°C$. Figure 6 shows the simulated output power from the 8×60 network as a function of the temperature gradient. As comparison, the simulated array output power corresponding to the equivalent average illumination (uniformly illuminated) as for the temperature gradient is shown. Figure 6 illustrates that the array output power decreases more rapidly under a temperature gradient than for the case of equivalent uniform illumination, despite the equivalent average illumination from the hot side. The larger the temperature gradient, the larger the deviation from the $T_{average}$ behavior, due to the networking losses discussed in the previous section. For a linear temperature gradient of $\Delta T=90°C$ the output power is reduced by 27Watts (~32% relative decrease in power) compared to the fully illuminated array. The corresponding decrease in power from the uniformly irradiated array having equivalent average illumination as for the 90°C temperature gradient shows a ~23% relative decrease. Thus an additional ~8% relative decrease in power density/efficiency due to the networking losses is predicted for $\Delta T=90°C$.

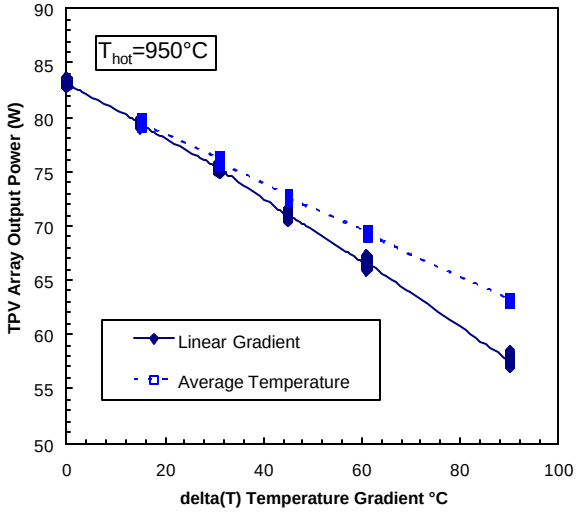

FIGURE 6. Simulated network output power from an 8×60 array of TPV diodes as a function of temperature gradient and uniformly illuminated case having an average temperature

INFLUENCE OF REVERSE BREAKDOWN FOR A CONTINUOUS TEMPERATURE GRADIENT

A slowly varying temperature gradient will result in a large number of cells operating at slightly different points along their individual IV curve. In this section we reconsider the distribution of diodes in a 8×60 array under a linear temperature gradient for different reverse breakdown parameters . Unlike the case of an abrupt gradient across a single diode, the array IV does not exhibit strong kinks for this network. The network's maximum power is not strongly affected by the reverse breakdown characteristics of this particular population. The shape of the network's IV-curves do however depend on the breakdown voltages. For low breakdown diodes, the array's I_{sc} is much greater than the I_{sc} of the high breakdown diodes,

however the fill factor is significantly less. In this case, as for the case of an abruptly shaded diode, the shape of the IV curves will strongly depend on whether the limiting diode(s) breakdown in the array's 4th or 3rd quadrant, corresponding to low FF/high I_{sc} or high FF/low I_{sc} respectively. Regardless of the shape of the IV curve in this case, the P_{max} is limited to the same value by the weakly illuminated diode(s). Figure 7 shows the 6×80 array's IV characteristics under full-uniform illumination (from the full population) and then re-simulated having different reverse breakdown characteristics under a 90°C temperature gradient. The breakdown properties simulated ranged from the highest to lowest in Figure 4 . In figure 7, the top-right-hand quadrant is the power generating 4th quadrant. The maximum power point is observed to remain independent of the reverse characteristic, however the array short circuit current and fill factor do not. Note that the array reverse breakdown occurs at currents approximately equal to the light generated current of the maximum illuminated cell (i.e. all other diode have broken down to support the highest I_{light}.

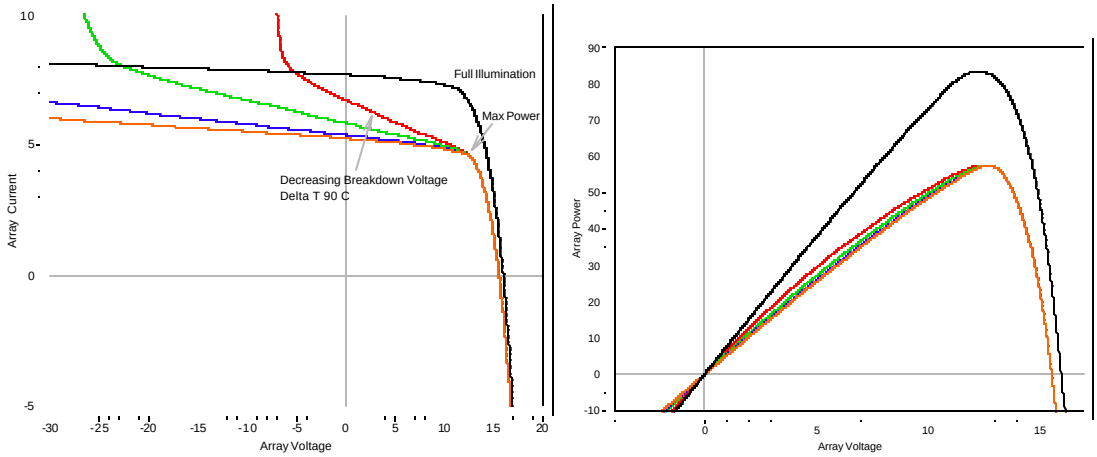

FIGURE 7. Simulated Current Voltage characteristics (left) of a full-uniform illumination 6×80 array (black) and under a 90°C temperature gradient. The influence of four reverse breakdown characteristics is depicted in the figure. The second figure shows the corresponding Power-Voltage curves.

DEPOSITION

Long term operation of a TPV system will cause some level of deposition on the cold side system components (i.e., filters/diodes) that acts to degrade the light generated current in the diode. In the general case, deposition will be non-uniform, being the most severe in the vicinity of the hottest parts of the radiator. Figure 8 shows a hypothetical deposition profile for a TPV system, having non-uniform axial distribution caused by a radiator temperature gradient. Knowledge of vapor pressure curves for typical high purity solids (we used the vapor pressure curves for Si in this case) are used to predict the end-of-life obscuration as a function of temperature, which are then normalized to 10% maximum obscuration across from the hottest section.

Simulations show that maximum output power is 54.5W after deposition. This corresponds to approximately 2.5W decrease in power, representing a 5% loss. Note that the obscuration profile will act to mitigate the current mismatch associated with the beginning-of-life temperature gradient.

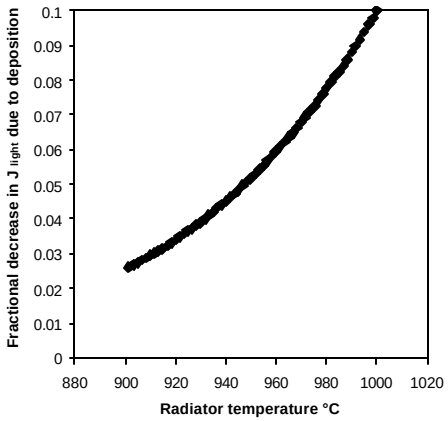

FIGURE 8. Hypothetical obscuration profile, representing the end-of-life obscuration of useful radiant power to the diode.

CONDUCTION LOSSES IN TPV SYSTEMS

If a vacuum environment is not maintained, then parasitic conduction losses will occur from hot side to cold side. As opposed to radiative heat transfer, all conduction heat transfer will manifest purely as an efficiency degradation. In addition, structural supports may also conduct heat parasitically from hot side to cold side, thus thermal contact between radiator and cold side must be minimized in any system design.

The thermal to electric efficiency is defined as the ratio of electrical power output P_{elec} (W_e/m^2) to the total heat power $Q_{absorbed}$ absorbed by the diode array (W_Q/m^2). A TPV generator which is contained in an ambient gas and having thermally conductive structural support will transfer additional heat energy parasitically from the hot side to the surroundings. In this case the efficiency is degraded according to equation (3).

$$\eta_{system} = \frac{P_{elec}}{Q_{absorbed}} = \frac{P_{elec}}{Q_{rad}} \times \frac{Q_{rad}}{Q_{rad} + Q_{conductive}^{Gas} + Q_{conductive}^{structural}} = \eta_{TPV} \times \eta_{Radiative} \qquad (3)$$

Where η_{TPV} is the radiative conversion efficiency and $\eta_{radiative}$ is the ratio of radiative heat transferred to total heat transferred from hot side to cold side. In this paper, thermal conductance across either N_2 or Xe, are considered where the average thermal conductivities for N_2 and Xe are taken to be ~0.5mWcm^{-1}K^{-1} and 0.12mWcm^{-1}K^{-1} at $T_{average}$ ~600K. Figure 9 shows $\eta_{radiative}$ as a function of distance between hot and cold side for the two ambient gases considered. Typical spacing is generally on the order of a few mm.

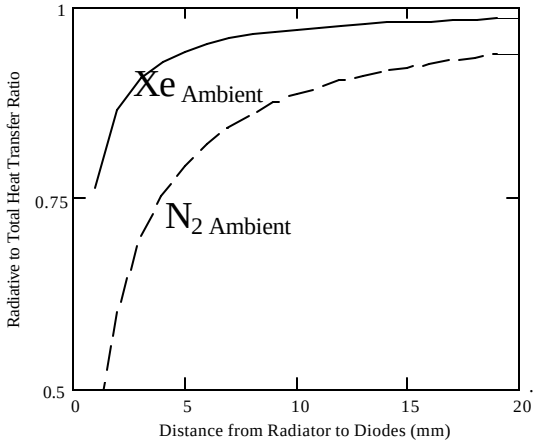

FIGURE 9. The ratio of radiative heat transfered to total heat transfered from hot side to cold side as a function of distance between hot and cold sides, and for two different gas ambients.

OPTICAL CAVITY EFFECTS

The above analyses had assumed radiation heat transfer between two infinite parallel, diffuse, grey plates which is a reasonable assumption for large area plates, but neglects the following effects associated with an actual finite size TPV energy conversion system:

- Photon losses at the boundaries.
- Anisotropic optical properties of the TPV cell/filter surfaces.

As a preliminary analysis, these effects were estimated with an optical analysis of solid models using TracePro® from Lambda Research Corporation. The resulting map of irradiance reaching the active region of TPV diodes is shown in Figure 10. The results shown in Figure 10 are based on the following assumptions:

- 800-1000°C uniaxial, radiator temperature gradient.
- Measured SiC directional, spectral emittance at 500°C for the radiator.
- 120 x 80 mm finite size radiator and TPV cell surface.
- 2 mm gap between the radiator and the TPV cell surface.
- Anisotropic reflectance of the TPV cell using a grid with reflectance of 85% of the area based on measured directional, spectral reflectance of a front surface, tandem filter and reflectance of Au for the remaining 15% of the area.

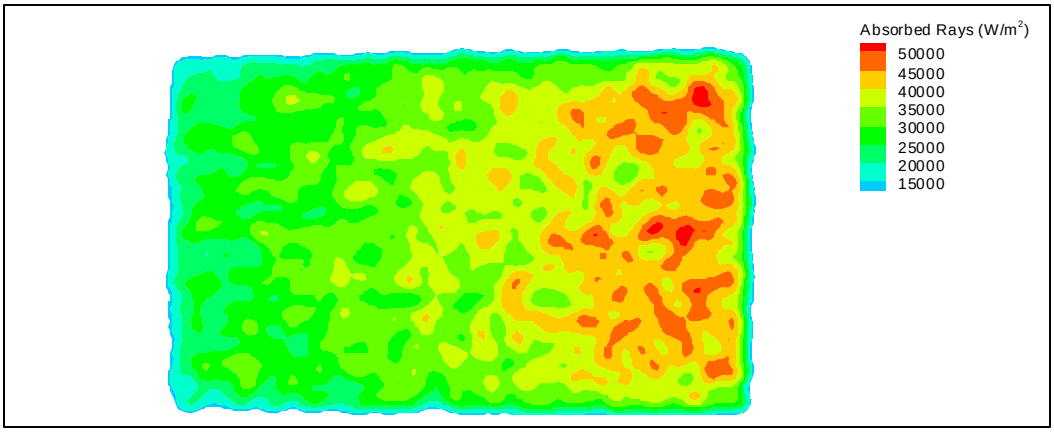

FIGURE 10. Total Irradiation absorbed within the TPV array

The resulting irradiance reaching the TPV diodes is far from uniform as expected. The absorbed power varies spatially by nearly a factor of two. The absorbed radiant power as a function of temperature gradient follows that predicted from the infinite parallel plate approximation, with the exception of a sharp drop-off in absorbed power near the plate edges. This sharp edge drop off must be alleviated/accommodated in system design, otherwise diodes in the vicinity of the edges will be abruptly mismatched as discussed in Section IVa.

SUMMARY OF POTENTIAL LOSS NETWORKING LOSSES

The previous sections discussed the individual networking/system losses in TPV generators, many of which can be treated independently, at least to first order. Component variability and non-uniform illumination/cavity effects are expected to each contribute a 10% relative efficiency loss. Network design will require knowledge of generator's spatial illumination profile (i.e. abrupt vs. weakly varying illumination gradients). In addition, thermal conduction losses across ambient gases are also predicted to reduce efficiency by approximately 10 relative percent. This corresponds to a beginning-of-life TPV system efficiency on the order of 15% system efficiency, depending on system design specifications.

Reductions in performance due to end-of-life deposition is anticipated to provide an end-of-life system efficiency of approximately 13-14% using current technology. These predictions are rough estimates, as many of the simulations/assumptions have not been experimentally verified, nor does a unique system design exist. Table III summarizes the nominal networking losses associated with the items discussed in this paper. Highest system performance will require a tightly controlled manufacturing environment, as well as network design to mitigate the losses listed in Table III..

Table III. Summary of Networking/System Losses in a TPV Generator

Networking Factor	Relative Power/Efficiency Loss	Efficiency	Near Term ~5 year	Design Options
Small Scale efficiency	0%	~20% [1]	~25%	Diode/Filter Improvements
Component Variability	~10%	18%	22.5%	•Set by selection criteria / cost
Temperature/Illumination Gradients	~10%	~16%	20%	•Minimize non-uniformity, • Reverse breakdown •Adjust diode size to accommodate current mismatch
Thermal Conductance/Convection	~10%	~15%	18%	•In-vacuum ambient •Minimize Support Structures
Deposition	~5%	14%	17%	•Low vapor pressure radiators • Environmental Control

REFERENCES

[1] B. Wernsman, R.R. Siergiej, S.D. Link, R.G. Mahorter, M.N. Palmisiano, R.J. Wehrer, R.W. Shultz, R.L. Messham, S. Murray, C.S. Murray, F. Newman, D. Taylor, D. Depoy, and T. Rahmlow " Greater than 20% Radiant Heat Conversion Efficiency of a Thermophotovoltaic Radiator/Module System Using Reflective Spectral Control", IEEE Trans. Elec. Dev., vol. 51, no. 3, pp. 512-516, (2004).

[2] M. W. Dashiell, et al. "0.52eV Quaternary InGaAsSb Thermophotovoltaic Diode Technology" To be presented at the The Sixth Conference on Thermophotovoltaic Generation of Electricity, June 14-16, 2004 in Freiberg, Germany.

[3] T.D. Rahmlow, "Design Considerations and Fabrication Results for Front Surface TPV Spectral Control Filters", To be presented at the The Sixth Conference on Thermophotovoltaic Generation of Electricity, June 14-16, 2004 in Freiberg, Germany.

[4] L.R. Danielson, et al. "Measurement Techniques for Single Junction Thermophotovoltaic Cells", Proceedings Fourth NREL Conference, Thermophotovoltaic Generation of Electricity, pp. 317-326 (1999).

[5] H.S. Rauschenbach, "Solar Cell Array Design Handbook, Principles and Technology of Photovoltaic Energy Conversion", Van Nostrand Reinhold Co., New York, 1980.